Environ Sci Pollut Res (2015) 22:17031–17040
DOI 10.1007/s11356-015-4839-2

RESEARCH ARTICLE

Insights into tetracycline adsorption onto kaolinite and montmorillonite: experiments and modeling

Yanping Zhao[1] · **Xueyuan Gu**[2] · **Shiyin Li**[1] · **Ruiming Han**[1] · **Guoxiang Wang**[1]

Received: 31 March 2015 / Accepted: 3 June 2015 / Published online: 28 June 2015

Abstract Adsorption of tetracycline (TC) on kaolinite and montmorillonite was investigated using batch adsorption experiments with different pH, ionic strength, and surface coverage. As a result, pH and ionic strength-dependent adsorption of TC was observed for the two clay minerals. The adsorption of TC decreased with the increase of pH and ionic strength, and high initial TC concentration had high adsorption. In addition, a triple-layer model was used to predict the adsorption and surface speciation of TC on the two minerals. As a result, four complex species on kaolinite ($\equiv X^- H_3TC^+$, $\equiv X^- H_2TC^\pm$, $\equiv SOH^0 H_2TC^\pm$, and $\equiv SOH^0 HTC^-$) and three species on montmorillonite ($\equiv X^- H_3TC^+$, $\equiv X^- H_2TC^\pm$, and $\equiv SOH^0 HTC^-$) were structurally constrained by spectroscopy, and these species were also successfully fitted to the adsorption edges of TC. Three functional groups of TC were involved in these adsorption reactions, including the positively charged dimethylamino group, the C=O amide I group, and the C=O group at the C ring. Combining adsorption experiments and model in this study, the adsorption of TC on kaolinite and montmorillonite was mainly attributed to cation exchange on the surface sites ($\equiv X^-$) compared to surface complexation on the edge sites ($\equiv SOH$) at natural soil pH condition. Moreover, the surface adsorption species, the corresponding adsorption modes, and the binding constants for the surface reactions were also estimated.

Keywords Tetracycline · Adsorption · Kaolinite · Montmorillonite · Surface complexation model

Responsible editor: Marcus Schulz

Electronic supplementary material The online version of this article (doi:10.1007/s11356-015-4839-2) contains supplementary material, which is available to authorized users.

✉ Guoxiang Wang
wangguoxiang@njnu.edu.cn

Yanping Zhao
yanping-zhao@163.com

Xueyuan Gu
xueyuangu@126.com

Shiyin Li
Lishiyin88@126.com

Ruiming Han
hanruiming12@126.com

[1] Jiangsu Key Laboratory of Environmental Change and Ecological Construction, Jiangsu Center for Collaborative Innovation in Geographical Information Resource Development and Application, School of Geographical Science, Nanjing Normal University, 1, Wenyuan Road, Xianlin University District, Nanjing 210023, China

[2] State Key Laboratory of Pollution Control and Resource Reuse, School of the Environment, Nanjing University, Nanjing 210023, China

Introduction

Tetracyclines (TCs), one of the most widely used antibiotic families in the world, are widely used in human therapy and livestock industry (Sarmah et al. 2006). However, 50–80 % of TCs cannot be absorbed or metabolized in vivo and are finally released unchanged in excreta (Bound and Voulvoulis 2004). Due to the application of animal wastes as plant nutrient sources and soil amendments, TCs can accumulate in soil to the level of mg kg^{-1} (Hu et al. 2008). Frequent application of TCs has raised emerging threat to ecological safety and human health, such as the adverse effects on soil microbial (Thiele-Bruhn and Beck 2005) and aquatic photosynthetic organisms (Wilson et al. 2004), as well as triggering of the dissemination of antibiotic-resistant genes (Knapp et al. 2010). All these

mentioned above make studies of the interactions between TCs and soils (or minerals) increasingly important.

The behavior of TCs in soils is closely related to their adsorption-desorption characteristics, which depend on the molecule structure and function groups. TCs are amphoteric molecules, which have multiple ionizable functional groups. Taking the TC molecule for example, there are three major functional groups, such as the tricarbonylamide group, phenolic diketone group, and dimethylamino group (Fig. S1). TCs can undergo protonation-deprotonation reactions and present different species depending on the solution pH (Fig. S2), like cationic form (H_3TC^+) at pH<3.3, zwitterionic form ($H_2TC^{\pm}$) at 3.3<pH<7.68, or anionic form (HTC^-, TC^{2-}) at pH>7.68 (Fig. S2) (Parolo et al. 2008). Many batch and spectroscopic studies have been conducted to reveal the pH-dependent sorption of TCs onto different materials, including phyllosilicate clays (Pils and Laird 2007), oxide minerals (Figueroa and Mackay 2005), humic substances (Gu et al. 2007), clay-humic complexes (Gu and Karthikeyan 2008), and soils (Carrasquillo et al. 2008). It has been demonstrated that TCs can be sorbed onto phyllosilicate clays via cation exchange (Pils and Laird 2007), cation bridging (Figueroa et al. 2004), or surface complexation (Figueroa et al. 2004). Although many studies have been conducted to reveal the interaction between TC and soil minerals, knowledge about the surface adsorption speciation on minerals is still limited. Thus, it is extremely important to establish a comprehensive model to describe the adsorption species of TC on clay minerals, which will direct toward better understanding the mechanism of adsorption of TC onto clay minerals.

Surface complexation models (SCMs) are thermodynamic approaches to describe the formation of surface adsorption species between dissolved solutes and surface functional groups. These models have been widely used to describe the surface adsorption behavior, especially for the adsorption of heavy metals to minerals (Gu and Evans 2008; Lund et al. 2008). In the last decade, SCMs have also been successfully applied to study the sorption behaviors of ionic organics on oxide minerals, which contain several kinds of variable charge edge sites. A two-layer model was used to predict the adsorption of a series of organic acids onto goethite (Evanko and Dzombak 1999). The basic stern model (BSM) was applied to investigate the adsorption of glyphosate on goethite (Jonsson et al. 2008). However, little information is available for the application of SCMs to study the sorption process on soil clay minerals. Therefore, it is interesting and anticipated to apply the SCMs to predict TC adsorption and surface speciation on soil minerals.

Soil clays are the most important adsorbents for TC in soils due to their high abundance, large specific surface area, negative charge, and hydrophilic surface (Morton et al. 2001). Among the soil clays, kaolinite and montmorillonite are especially important because of their widespread occurrence in soils (Liu et al. 2008). Different structures of kaolinite and montmorillonite can directly lead to a range of different physical properties, including surface area, cation exchange capacity (CEC), and point zero of charge (pH_{zpc}). All these properties can exert a profound influence on the final fate of TC in the soil environment. The aim of this work is to develop an SCM to predict TC adsorption and surface speciation on kaolinite and montmorillonite under wide conditions of pH, ionic strength, and surface coverage and reveal the mechanism of TC adsorption onto clay minerals.

Materials and methods

Materials and chemicals

TC (96 % purity) was purchased from Sigma-Aldrich Co. (St. Louis, MO, USA). Acetonitrile (HPLC grade) and oxalic acid (99 % purity) used as HPLC mobile phase for analyzing TC were also purchased from Sigma-Aldrich Co. All other chemicals were of analytical grade (Sinopharm Chemical Reagent Co.). Deionized water (resistivity=18.2 MΩ cm^{-1}) was used throughout this study.

The samples of kaolinite and montmorillonite used in this study were obtained from the south of Nanjing, China, and Upton, WY, USA (distributed by Ward's Natural Science Establishment, Inc.), respectively. The preparation of sorbents was conducted according to the previous study (Zhao et al. 2011). The specific surface area of kaolinite and montmorillonite was 22.3 and 46.0 m^2 g^{-1}. The CEC of these two minerals was 0.140 and 0.705 mol kg^{-1} at pH 4 and 0.159 and 0.908 mol kg^{-1} at pH 8, respectively.

Batch adsorption experiments

The effects of pH and ionic strength on TC adsorption onto kaolinite and montmorillonite were examined using batch experiments in 0.001, 0.01, and 0.1-M $NaNO_3$ solution at equilibrium pH 3–10. All the adsorption experiments were conducted using 22-mL glass vials equipped with polytetrafluoroethylene-lined screw caps. The solid-to-water ratio for the TC-kaolinite and TC-montmorillonite system was 1 and 0.2 g L^{-1}, respectively. The initial concentration of TC was 0.113 mM. The samples were mixed on a reciprocal shaker at 150 rpm, 25±0.5 °C for 24 h. N_2 was purged to remove dissolved oxygen to avoid possible oxygen-mediated degradation of TC (Ji et al. 2009). The equilibrium pH values were measured immediately at the end of the equilibrated time using an Orion 8272 PerpHect Ross Sure-Flow electrode. Then, the suspension was centrifuged and TC in the supernatant was analyzed using HPLC. The detailed procedure is described in references (Zhao et al. 2011, 2012). To take account of solute loss from processes other than

adsorbent sorption, calibration curves were built separately at the same treatment and conditions (pH, temperature, equilibration time, etc.) as the adsorption samples without adsorbent. Before being detected by HPLC, the pH values of adsorption samples and calibration curve samples were all adjusted to 2.5 using diluted HNO_3 solution. The effects of surface coverage on TC adsorption onto kaolinite and montmorillonite as a function of pH were conducted similar to the above method except the initial TC concentrations.

ATR-FTIR measurements

Attenuated total reflectance-Fourier transform infrared (ATR-FTIR) spectra were collected using a Vertex 70-V FTIR spectrometer (Bruker, Germany) equipped with a liquid-nitrogen-cooled MCT detector and a 022-2020 ZnSe crystal fitted in a horizontal attenuated total reflectance (HATR) cell (Pike Technologies). A total of 256 scans with a spectral resolution of 4 cm^{-1} were employed.

TC solutions (0.5 mM) within 1 g L^{-1} kaolinite and 0.2 g L^{-1} montmorillonite suspension were prepared at different equilibrium pH values (pH 3, 5, 7, 8, and 10) adjusted with $NaOH/HNO_3$, respectively. $NaNO_3$ solution (0.01 M) was used as background electrolyte. The samples were wrapped in aluminum foil to prevent exposure to light and shaken for 24 h at 150 rpm, 25±0.5 °C. After equilibrium, the tubes were centrifuged for 30 min at 2880*g*, and the solid and supernatant were collected separately and immediately spread on the ZnSe crystal surface to obtain a thin layer. Then, FTIR spectra were measured. Spectra of kaolinite and montmorillonite in 0.01 M $NaNO_3$ were also obtained at five identical pH values in the absence of TC, respectively. Difference spectra attributable only to the TC-clay surface complexes were obtained by subtracting the supernatant and clay-$NaNO_3$ suspension signals from the corresponding spectra of the solid. For the spectra of aqueous TC at different pH values, the spectral contributions from water were removed by subtraction of the spectrum of the background electrolyte solution (at the same pH) from the TC spectrum.

Surface complexation modeling

Both kaolinite and montmorillonite contain permanent negative charge surface functional groups ($\equiv X^-$) arising from isomorphous substitution or nonideal octahedral occupancy. In addition, these two minerals also have variable-charge edge hydroxyl groups (≡SOH, where S is Si or Al), which can undergo protonation ($\equiv SOH_2^+$) and deprotonation ($\equiv SO^-$) as a function of the solution pH. A triple-layer model (TLM) was used to predict the surface electrostatic properties of kaolinite and montmorillonite in the present study using a least squares fitting program FITEQL version 4.0 (Herbelin and Westall 1999). The TLM allows adsorption to occur in three surface planes (Essington et al. 2010). Protons and specifically adsorbed species (metals and ligands) are retained in the o plane, and the adsorbed species containing hydrated waters are retained in the β plane. These two planes are enveloped by a diffuse layer (d plane), where counterions are retained to balance the charge in the o and β planes. The TLM enables consideration of the type of electrolytes and concentrations, and the model accounts for the surface complex structures, which cannot be described by constant capacitance or diffuse layer models (Dzombak and Morel 1990). The TLM requires several parameters, including the surface protonation equilibrium constants ($\log K_{(\equiv SOH2+)}$ and $\log K_{(\equiv SO-)}$), the electrolyte adsorption equilibrium constants ($\log K_{(\equiv SOH2+\ NO3-)}$, $\log K_{(\equiv SO-\ Na+)}$, and $\log K_{(\equiv X-\ Na+)}$), the specific surface area (A_S), the concentration of basal sites and edge sites (N_t), and the inner- and outer-layer capacitance (C_1 and C_2).

The equilibrium constants $K_{(\equiv SOH2+)}$, $K_{(\equiv SO-)}$, $K_{(\equiv SOH2+\ NO3-)}$, $K_{(\equiv SO-\ Na+)}$, and $K_{(\equiv X-\ Na+)}$ and layer capacitance C_1 and C_2 for kaolinite and montmorillonite could be estimated through the fitting for titration data at different ionic strengths with the FITEQL program (Goldberg 2005; Landry et al. 2009). Besides, the site density (N_t) is a critical parameter for TLM. For the permanently charged site $\equiv X^-$, it is normally obtained by measuring the CEC (Essington et al. 2010). However, accurate estimates of the edge site densities remain uncertain (Bourg et al. 2007) and are usually obtained either from potentiometric titrations (Baeyens and Bradbury 1997) or optimized by FITEQL or other similar programs (Ikhsan et al. 2005). In this study, the total site densities of both permanent and edge sites for kaolinite and montmorillonite were assumed equal to the CEC value measured at pH 8 (0.159 and 0.908 mol kg^{-1}, respectively). The basal site densities for the corresponding mineral were assumed to be equal to the CEC measured at pH 4 (0.140 and 0.705 mol kg^{-1}, respectively). The goodness-of-fit parameter (V_y) computed by FITEQL was determined by the ratio of weighted sum of squares and the degrees of freedom (WSOS/DF). The values between 0.1 and 20 are considered as a reasonable fit to the experimental data (Swedlund et al. 2009).

Results and discussion

Adsorption edges of TC onto kaolinite and montmorillonite

Effects of ionic strengths (0.001, 0.01, and 0.1 mol L^{-1} $NaNO_3$) and equilibrium pH (range of 3 to 10) on the adsorption of TC onto kaolinite and montmorillonite were investigated by batch adsorption experiments (Fig. 1). As a result, the adsorption of TC was significantly affected by solution pH and ionic strength, but the adsorption behaviors were different for the two minerals.

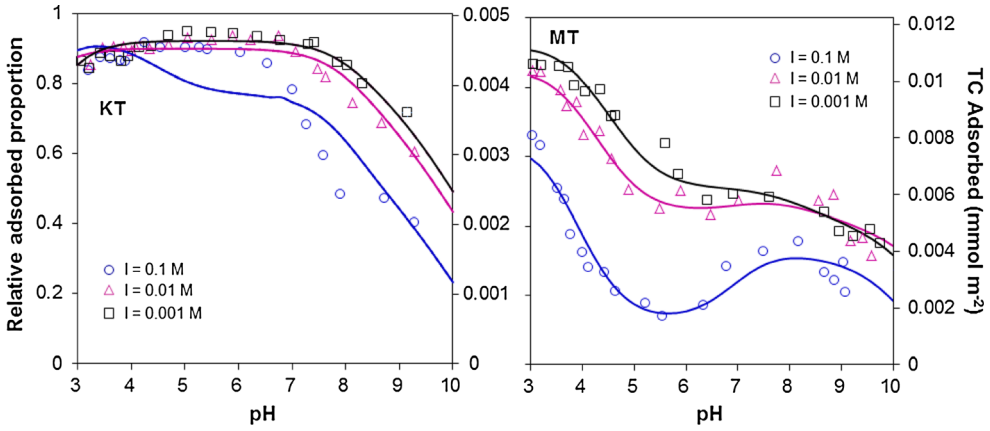

Fig. 1 Adsorption edges of TC on kaolinite (KT, 1 g L^{-1}) and montmorillonite (MT, 0.2 g L^{-1}) at different ionic strengths, 25 °C. Total concentration of TC 0.113 mM, equilibration time 24 h. The *dots* are experimental data and *solid lines* represent the model predicted using parameters in Table 1

The TC adsorption saturation on kaolinite was observed at pH 3–6, followed by a dramatic decrease as pH and ionic strength is increasing (Fig. 1). These trends were consistent with previous studies (Figueroa et al. 2004; Wang et al. 2010). At pH<3.3, the predominant form of TC is a cation (H_3TC^+, Fig. S2) which can be adsorbed by negatively charged surface sites of clay through cation exchange (Figueroa et al. 2004; Zhao et al. 2011). With pH increasing, TC adsorption decreased due to the increase of electrostatic repulsion between the deprotonated TC forms (Fig. S2) and the negatively charged sites of clay (Wang et al. 2010). However, the TC adsorption on kaolinite was almost unchanged at pH 3–6 and the sorption amounts did not exhibit a characteristic shape "edge" but made up over 40 % of the total amounts even at pH 9 (Fig. 1), where TC anion dominates fully (Fig. S2). These results indicated that the zwitterionic form of TC ($H_2TC^{\pm}$) should be involved in the cation exchange on the negatively charged surface sites, and the surface complexation on edge sites was expected to be another important mechanism other than the cation exchange reaction (Essington et al. 2010; Figueroa et al. 2004; Wang et al. 2010).

Different from the adsorption on kaolinite, the adsorption curves of TC on montmorillonite presented a great decrease at pH<6 with three ionic strengths (Fig. 1). A local maximum was reached at around pH 8, followed by a gradual decrease (8<pH<9). These trends were consistent with previous studies (Figueroa et al. 2004; Parolo et al. 2010; Wang et al. 2008). At pH 3–6, the positive charge of the TC molecule decreased with the deprotonation of the tricarbonylamide group (Fig. S2), which led to the reduction of the cation exchange on the permanent negatively charged surface of montmorillonite and the consequent depressed adsorption. As pH>6, the phenolic diketone group in the TC molecule began to deprotonate (Figs. S1 and S2). There might be two different processes impacting the adsorption. On one hand, TC adsorption might be inhibited because of the decreased cation exchange. On the other hand, the adsorption could be improved due to the surface complexation between the deprotonated functional groups of TC and the variable charged edge sites of montmorillonite (Figueroa and Mackay 2005). Specially, the tricarbonylamide group has higher steric hindrance from the dimethylamino group, compared with the phenolic diketone group (Zhao et al. 2012). Hence, the phenolic diketone group may be the major site complex with montmorillonite edge sites under alkaline condition. This may be why the small adsorption peak presented at around pH 8, where the phenolic diketone group started to become dominant (Fig. S2). As pH is increasing, the electrostatic repulsion between TC and montmorillonite increased and the adsorption was inhibited. Accordingly, the cation exchange on surface sites and the surface complexation on edge sites both contributed to the adsorption of TC on montmorillonite.

Furthermore, the results also showed that TC exhibited greater sorption onto montmorillonite than onto kaolinite. In 0.01-M $NaNO_3$ solution with the pH of 3, 7.5, and 9, the amounts of TC adsorbed onto montmorillonite were 0.011, 0.0074, and 0.0047 mmol m^{-2}, respectively, while those of kaolinite were 0.0045, 0.0042, and 0.0031 mmol m^{-2} (Fig. 1). This result was consistent with previous studies (Carrasquillo et al. 2008; Figueroa et al. 2004; Pei et al. 2010). This may due to a much lower CEC and surface area, as well as the absence of any expandable clay interlayer regions for kaolinite relative to montmorillonite (Pei et al. 2010). Besides, it was also observed that the difference of TC adsorbed amounts onto the two kinds of clay became smaller as pH is increasing (Fig. 1), which suggested that the contribution of cation exchange on surface sites to TC adsorption on montmorillonite diminished at high pH values because of the reducing positive charge in the TC molecule.

It was found that ionic strength had great impacts on TC adsorption on kaolinite and montmorillonite (Fig. 1). TC adsorption on the two minerals was inhibited with the increasing ionic strength. At around pH 7.0, the amounts of TC adsorbed onto kaolinite and montmorillonite decreased from 0.0046 to 0.0061 mmol m^{-2} in 0.001-M $NaNO_3$ solution to 0.0039 and 0.0036 mmol m^{-2} in 0.1-M $NaNO_3$ solution, respectively. This trend was consistent with previous reports (Figueroa et al. 2004; Kulshrestha et al. 2004). Besides, higher ionic

strength, larger ionic radius and higher cation valence decreased TC adsorption to clay minerals in our previous studies (Zhao et al. 2011, 2012). The presence of Na^+ ions might compete with the TC molecule for the surface negatively charged sites, which was strong evidence of cation exchange interaction and a possible outer-sphere adsorption mechanism.

For the adsorption of TC on montmorillonite, the low-pH portion was more sensitive to ionic strength than that of high-pH condition (Fig. 1). This may be because the cation exchange interaction on surface sites diminished and there is relatively increasing surface complexation on edge sites at high pH values (Zhao et al. 2012).

FTIR analysis of adsorbed TC

The ATR-FTIR spectra were investigated for the TC in electrolyte solution at different pH (3, 5, 7, 8, and 10) and the TC adsorbed onto different clay minerals at identical pH values. The most characteristic region of the TC spectrum (1150–1750 cm^{-1}) was selected and interpreted in detail (Fig. 2). Peak assignments for TC followed the previous studies summarized in Table S1.

The FTIR spectra of TC show a clear pH-dependent behavior (Fig. 2a). Firstly, at pH 2.8, an absorption peak (a) (at 1668 cm^{-1}) is assigned to the C=O of the amide group at C13 (Li et al. 2010a, b). As pH is increasing, the vibration at (a) disappeared due to the deprotonation of the tricarbonylamide group (Aristilde et al. 2010). Secondly, the frequency at 1579 cm^{-1} (c) corresponds to the C=O group at ring C (Li et al. 2010a), and the width increased with increasing pH value because of the possible impact of the deprotonation of the adjacent hydroxyl group. Thirdly, the absorption peak at 1400 cm^{-1} (f) represents the $–CH_3$ deformation vibration (Parolo et al. 2010). The vibration of (f) at pH 10 is apparently different from those at lower pH conditions, which can be attributed to the deprotonation of the dimethylamino group under extremely alkaline condition. Besides, the vibration bands at 1608 cm^{-1} (b), 1505 cm^{-1} (d), 1448 cm^{-1} (e), 1267 cm^{-1} (g), 1229 cm^{-1} (h), and 1186 cm^{-1} (i) are associated with the carbonyl group at ring A, C–C stretching, the N–H in the dimethylamino group, the amino C–N in the amide group, the C–N in the dimethylamino group, and the phenolic C–O group (Aristilde et al. 2010; Chang et al. 2009; Kulshrestha et al. 2004; Li et al. 2010a; Parolo et al. 2010), respectively (Fig. 2a).

The interaction between TC and the two minerals was investigated by comparing the spectra of adsorbed TC with those of free molecules in solution. Figure 2 shows that the FTIR spectra of TC-kaolinite (KT) and TC-montmorillonite (MT) are pH dependent. When TC was adsorbed on kaolinite, the C=O amide I stretching band (a) even at pH 3.1 and the band of C–N at C13 (g) at five pH conditions were both significantly suppressed compared to free TC (Fig. 2b).

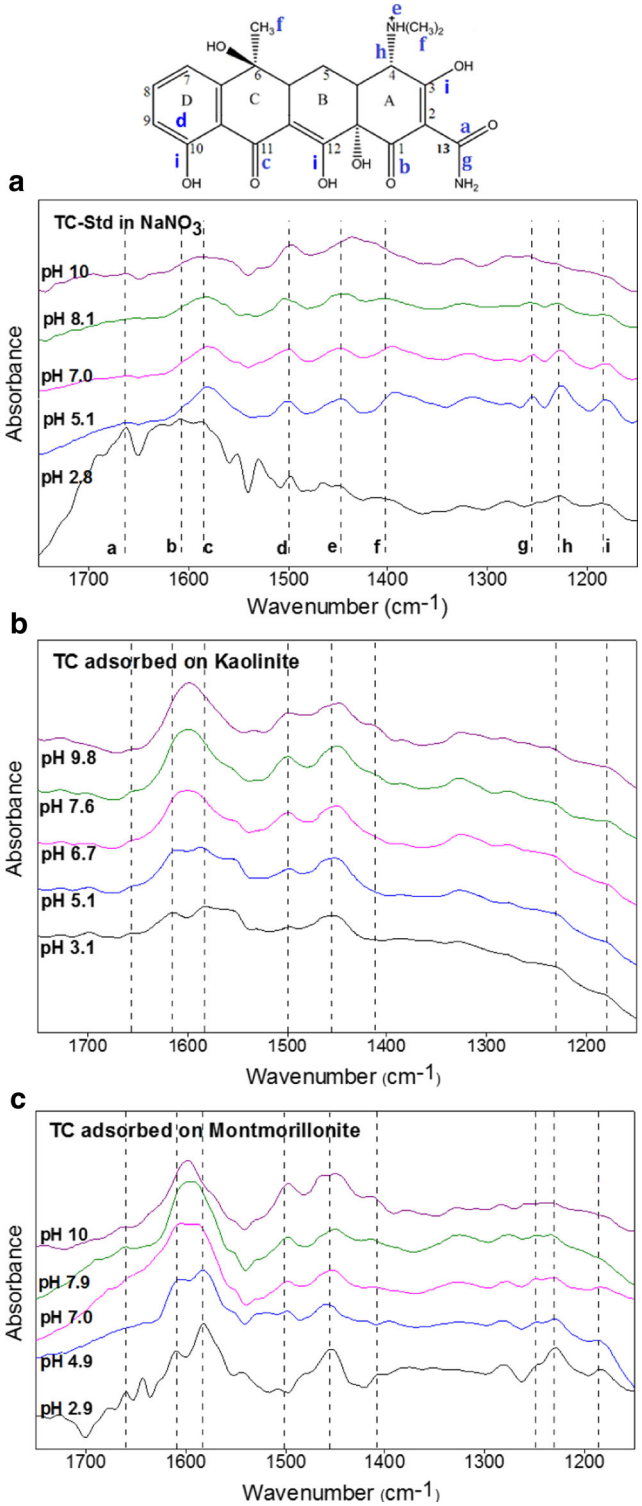

Fig. 2 ATR-FTIR difference spectra of aqueous TC (**a**), adsorbed TC on kaolinite (**b**), and adsorbed on montmorillonite (**c**) at different pH values. The TC structure shows the assigned IR vibration bands (**a** to **i**)

These results suggested that the C=O amide I group could bind to kaolinite almost over the whole studied pH range. In addition, compared to the spectrum for free TC, the vibration band at 1579 cm^{-1} (c) was inhibited after being adsorbed on

kaolinite at pH >6.7 (Fig. 2b), which indicated that the C=O group at ring C may contribute to the complex of TC with kaolinite under neutral to alkaline condition. By contrast, the vibration of the $–CH_3$ band (f) was significantly depressed at pH <7.6, and the frequencies shift from 1400 to 1414 cm^{-1} at 7.6 and pH 9.8. Meanwhile, the absorption peak of the N–H in the dimethylamino group (e) shifts from 1448 to 1459 cm^{-1}, indicating the involvement of the dimethylamino group during sorption to kaolinite. Thus, from the FTIR evidence, TC adsorption on kaolinite mainly occurred at the dimethylamino group (C4) and the C=O amide I group (C13) over a wide pH range and at the C=O group at ring C (C11) under neutral to alkaline condition. These results indicated that the cation exchange of the positively charged dimethylamino group in the TC molecule with the negatively charged surface sites and the surface complexation of the C=O amide I group and the C=O group at ring C with the variable charged edge sites are both important mechanisms of TC adsorption onto kaolinite.

Compared with kaolinite, the FTIR spectra of TC adsorbed on montmorillonite show a different result (Fig. 2c). The spectrum changes of vibration bands at the C=O group at ring C (c) and the dimethylamino group (N–H (e) and $–CH_3$ (f)) at different pH values were similar with the spectra of TC-KT (Fig. 2b). It should be noticed that the spectrum changes of vibration bands at the N–H and $–CH_3$ groups were much greater than the spectra of TC adsorbed on goethite (Fig. S3) determined in our previous study (Zhao et al. 2014). These results illustrated the important role of the dimethylamino group in TC adsorption on kaolinite and montmorillonite. Different from the spectra of TC-KT, vibration bands of TC-MT at the C=O amide I group (a) and the C–N at C13 (g) at five pH conditions were unchanged relative to the spectrum for free TC. Therefore, it could be estimated that TC adsorption on montmorillonite might be through the cation exchange of the dimethylamino group with permanent negatively charged surface sites over a wide pH range and the surface complexation of the C=O group at ring C (C11) under neutral to alkaline condition. The proposed adsorption sites in TC were inconsistent with the interpretation provided in Chang et al. (2009) and Parolo et al. (2010), which may be because of the impacts of drying the adsorption sample on the vibrational modes of the complex species and the lack of the spectrum information of TC standard at different pH values in these studies.

Surface complexation model

The TC adsorption edges were modeled using TLM by FITE QL. The major TLM parameters are listed in Table 1, including the surface protonation and electrolyte adsorption equilibrium constants of kaolinite and montmorillonite. These parameters are referring to previous studies, which are summarized in Tables S2 and S3. These parameters were then fixed and used in the adsorption edge experiments to estimate the values for the TC binding constants. A two-site model, including the permanent negatively charged surface site $\equiv X^-$ and the variable charged edge site ≡SOH (S stands for Al or Si) (Gu and Evans 2008; Ikhsan et al. 2004), was used in the TLM for TC adsorption edges.

The adsorption edges and the ATR-FTIR results suggested that there are probably four and three binding reactions for TC adsorption on kaolinite and montmorillonite, respectively. Thus, two species on the negatively charged surface sites $\equiv X^- H_3TC^+$ and $\equiv X^- H_2TC^\pm$ and two complexes on the edge sites $\equiv SOH^0 H_2TC^\pm$ and $\equiv SOH^0 HTC^-$ were used to fit TC adsorption edges on kaolinite. Meanwhile, $\equiv X^- H_3TC^+$, $\equiv X^- H_2TC^\pm$, and $\equiv SOH^0 HTC^-$ were applied to fit the adsorption edges on montmorillonite. The species/component matrix used to calculate the TC binding constants using the TLM is shown in Tables S4 and S5. The obtained parameters are summarized in Table 1, and predicted adsorption results are shown in Fig. 1. The goodness-of-fit parameters (V_y) for TC-kaolinite and TC-montmorillonite were 24.8, 2.3, and 1.9 and 15.6, 8.4, and 4.8 at 0.1, 0.01, and 0.001 M $NaNO_3$, respectively. Results indicated that both of the models for TC-kaolinite and TC-montmorillonite were capable of fitting the experimental results well over the entire pH range at three ionic strengths. The distribution of TC adsorption species on the two minerals at three different ionic strengths is shown in Fig. 3.

Model results showed that TC interacts with kaolinite mainly through four reactions (Eq. 9–12 in Table 1), and the major corresponding species were $\equiv SOH^0 H_2TC^\pm$, $\equiv SOH^0 HTC^-$, $\equiv X^- H_3TC^+$, and $\equiv X^- H_2TC^\pm$ (Fig. 3, KT). It was obvious that $\equiv X^- H_2TC^\pm$ and $\equiv SOH^0 H_2TC^\pm$ exist at the whole pH range. The amount of $\equiv X^- H_3TC^+$ reduced with increasing pH at around pH 3–6. The species $\equiv SOH^0 HTC^-$ appeared at pH 7 followed by gradual improvement as pH is increasing (Fig. 3, KT). In general, $\equiv X^- H_2TC^\pm$ was the dominant adsorption species over the entire pH range with different ionic strength, which indicated that the adsorption of TC on kaolinite was mainly attributed to the cation exchange interaction on surface sites compared with the surface complexation on edge sites. For TC adsorption on montmorillonite, $\equiv SOH^0 HTC^-$, $\equiv X^- H_3TC^+$, and $\equiv X^- H_2TC^\pm$ were the three major species over the studied range of pH and ionic strength (Fig. 3, MT). Similar with the former, the adsorption species $\equiv X^- H_2TC^\pm$ existed at the whole pH range, and $\equiv X^- H_3TC^+$ and $\equiv SOH^0 HTC^-$ formed at the acidic and alkaline condition, respectively.

Obviously, the results of the established model were extremely consistent with the evaluation from the adsorption experiments. Both the cation exchange on surface sites and the surface complexation on edge sites were the major adsorption mechanisms for TC adsorption onto clay minerals. Under acidic and neutral conditions, the cation exchange on surface

Table 1 Proposed triple-layer model (TLM) for TC adsorption onto kaolinite and montmorillonite

No.	Deprotonation of TC in solution[a]	log K^{0b}	
1	$H_2TC^{\pm}+H^+=H_3TC^+$	−3.30	
2	$H_2TC^{\pm}=HTC^-+H^+$	−7.68	
3	$H_2TC^{\pm}=TC^{2-}+2H^+$	9.68	
	Surface reaction	Kaolinite	Montmorillonite
4	$\equiv SOH^0+H^+=\equiv SOH_2^+$	5.00[c]	5.00[c]
5	$\equiv SOH^0=\equiv SO^-+H^+$	−11.2[c]	−11.2[c]
6	$\equiv SOH^0+H^++NO_3^-=\equiv SOH_2^+\cdot NO_3^-$	7.50[c]	7.50[c]
7	$\equiv SOH^0+Na^+=\equiv SO^-\cdot Na^++H^+$	−8.60[c]	−8.60[c]
8	$\equiv X^-\cdot H^++Na^+=\equiv X^-\cdot Na^++H^+$	−2.10[d]	−2.10[d]
	TC adsorption reaction[e]		
9	$\equiv SOH^0+H_2TC^{\pm}=\equiv SOH^0\cdot H_2TC^{\pm}$	9.81	–
10	$\equiv SOH^0+H_2TC^{\pm}=\equiv SOH^0\cdot HTC^-+H^+$	6.43	5.14
11	$\equiv X^-\cdot Na^++H^++H_2TC^{\pm}=\equiv X^-\cdot H_3TC^++Na^+$	7.70	8.58
12	$\equiv X^-\cdot Na^++H_2TC^{\pm}=\equiv X^-\cdot H_2TC^{\pm}+Na^+$	9.76	8.37

The TLM was used to account for complexation and electrostatic effects at the mineral surface. The capacitance of inner and outer Helmholtz layer for kaolinite and montmorillonite is 1.5 and 5 F m^{-2}

[a] Constants from reference (Figueroa et al. 2004)

[b] logK^0 was averaged from values in the three ionic strengths which were adjusted to zero ionic strength using the Davies equation (Gu et al. 2010)

[c] Constants from reference (Goldberg 2005)

[d] Constants from reference (Landry et al. 2009)

[e] Optimized from FITEQL in this work

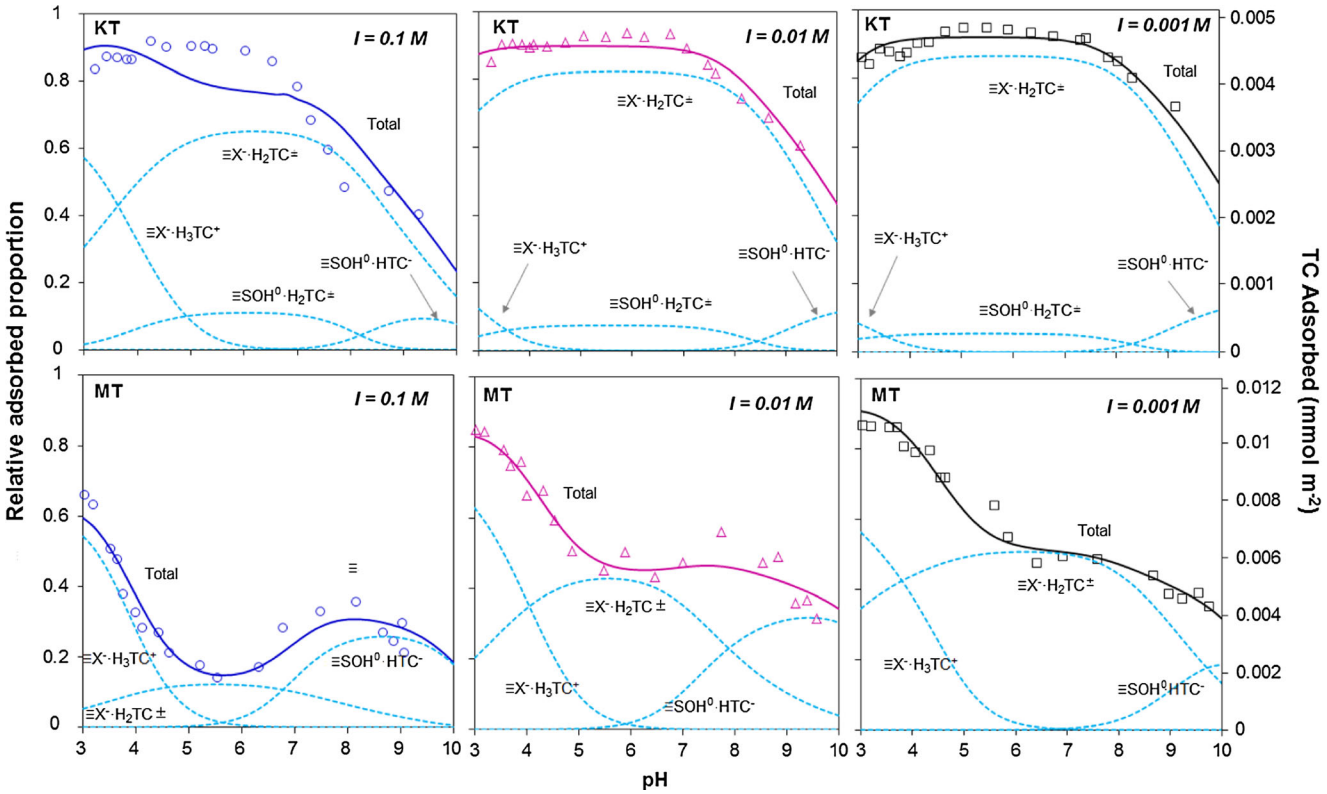

Fig. 3 Modeled surface speciation diagrams of TC adsorption onto kaolinite (KT, 1 g L^{-1}) and montmorillonite (MT, 0.2 g L^{-1}) at three ionic strengths, 25 °C. *Symbols* are experimental data and *lines* are fitted using the parameters in Table 1

sites predominantly contributed to the strong adsorption of TC on clay minerals instead of surface complexation. As pH is increasing, the dramatic decrease of positive charge in the TC molecule resulted in the inhibition of the cation exchange interaction on surface sites. However, the surface complexation on the edge sites enhanced gradually at high pH values,

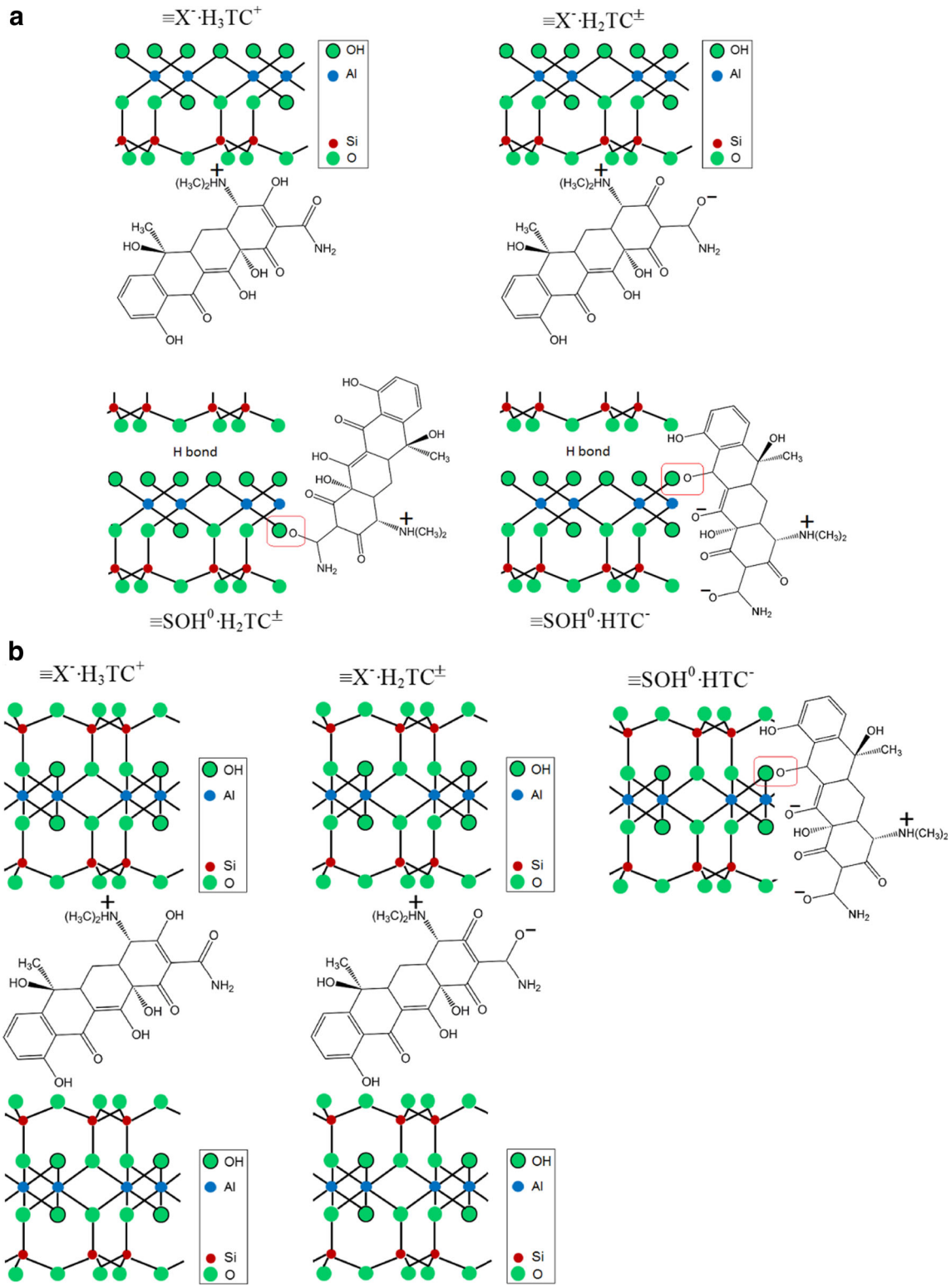

Fig. 4 Possible surface species representing different modes of TC attachment to kaolinite (**a**) and montmorillonite (**b**) surface sites, consistent with the surface complexation calculations in this study

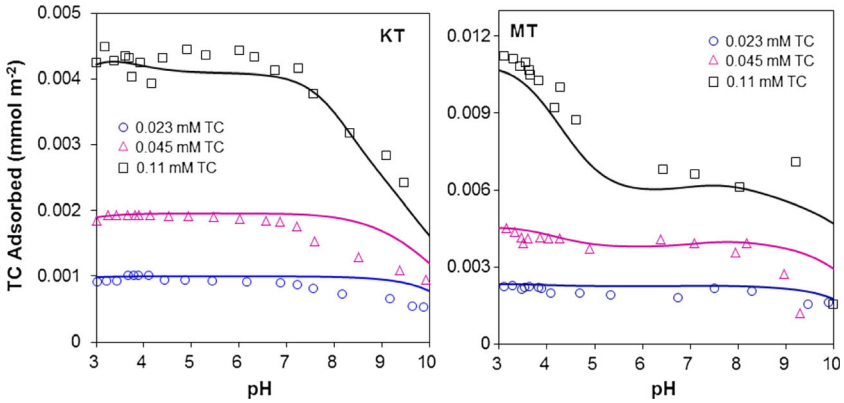

Fig. 5 Adsorption edges of TC with different initial concentration on kaolinite (0.023, 0.045, and 0.11 mM) and montmorillonite (0.11 and 0.23 mM), in 0.01-M $NaNO_3$ solution, 25 °C, and at 1 and 0.2 g L^{-1}, respectively. *Symbols* are experimental data and *lines* are fitted using the parameters in Table 1

which caused the presence of certain amounts of TC adsorbed even at extreme alkaline condition, especially for TC adsorption on montmorillonite.

According to the TC molecule and FTIR spectrum results, four coordinate modes of TC-kaolinite complexes (Fig. 4a) and three modes of TC-montmorillonite complexes (Fig. 4b) were proposed. For the TC-kaolinite, the negatively charged surface sites ($\equiv X^-$) can interact with the positively charged dimethylamino group (p*K*a=9.68) (C4) to form species $\equiv X^- H_3TC^+$ (pH 3–6) and $\equiv X^- H_2TC^\pm$ (whole pH range) through cation exchange with the pH-dependent presence of H_3TC^+ and $H_2TC^\pm$ (Fig. S2). In addition, over the studied pH range (pH 3–10), the existence of $H_2TC^\pm$ (Fig. S2) leads to the interaction of the variable edge sites ($\equiv SOH$) with the C=O amide I in the deprotonated tricarbonylamide group to form $\equiv SOH^0 H_2TC^\pm$ through surface complexation. Under neutral to alkaline condition, the edge sites can also complex with the C=O group (C11) in the deprotonated phenolic diketone group to form $\equiv SOH^0 HTC^-$. For the TC-montmorillonite condition, the distributions of the three species were similar with the TC-kaolinite except the absence of $\equiv SOH^0 H_2TC^\pm$. All these results demonstrated that the prediction of the TLM model were reasonable in this study.

Model validation

In order to test the applicability of the model established above, batch adsorption of TC on the two clay minerals was conducted with different initial concentrations (0.023, 0.045, and 0.11 mM) and pH values (range of 3 to 10). The experimental data were predicted using the parameters in Table 1, and the results showed that the prediction was reasonably good (Fig. 5). Predicted surface species for TC-kaolinite and TC-montmorillonite at three surface covers is shown in Fig. S4. These results showed that the models established in this study are relatively robust to predict the TC adsorption on kaolinite and montmorillonite under different ionic strength, pH, and surface coverage.

Conclusions

In this study, batch experiments and SCM were used together to reveal the adsorption of TC on clay minerals. Adsorption edge results showed that the adsorption of TC on the two minerals were pH and ionic strength dependent and exhibited greater adsorption on montmorillonite than on kaolinite. The ATR-FTIR spectroscopic evidence indicated that the positively charged dimethylamino group, the amide C=O, and the C=O at ring C were involved in TC adsorption on clay minerals. TLM was then developed to fit the macroscopic batch experimental data on kaolinite and montmorillonite. Four surface species ($\equiv X^- H_3TC^+$, $\equiv X^- H_2TC^\pm$, $\equiv SOH^0 H_2TC^\pm$, and $\equiv SOH^0 HTC^-$) on kaolinite and three species ($\equiv X^- H_3TC^+$, $\equiv X^- H_2TC^\pm$, and $\equiv SOH^0 HTC^-$) on montmorillonite could successfully fit all data at different pH, ionic strength, and surface coverage. The binding constants for the surface reactions were estimated, and the surface complexation modes were proposed. The adsorption of TC on kaolinite and montmorillonite was mainly attributed to cation exchange on the surface sites compared to surface complexation on the edge sites at natural soil pH condition. The results of this study will provide new insights into the adsorption process and surface speciation of TC on kaolinite and montmorillonite.

Acknowledgments This study was financially supported by the National Natural Science Foundation of China (No. 21407076), the Jiangsu Taihu Lake Water Environment Management Research (No. TH2014402), and the Jiangsu Natural Science Foundation (BK2011016)

References

Aristilde L, Marichal C, Miehe-Brendle J, Lanson B, Charlet L (2010) Interactions of oxytetracycline with a smectite clay: a spectroscopic study with molecular simulations. Environ Sci Technol 44:7839–7845

Baeyens B, Bradbury MH (1997) A mechanistic description of Ni and Zn sorption on Na-montmorillonite.1. Titration and sorption measurements. J Contam Hydrol 27:199–222

Bound JP, Voulvoulis N (2004) Pharmaceuticals in the aquatic environment-a comparison of risk assessment strategies. Chemosphere 56:1143–1155

Bourg IC, Sposito G, Bourg ACM (2007) Modeling the acid–base surface chemistry of montmorillonite. J Colloid Interface Sci 312:297–310

Carrasquillo AJ, Bruland GL, Mackay AA, Vasudevan D (2008) Sorption of ciprofloxacin and oxytetracycline zwitterions to soils and soil minerals: influence of compound structure. Environ Sci Technol 42:7634–7642

Chang PH, Li ZH, Jiang WT, Jean JS (2009) Adsorption and intercalation of tetracycline by swelling clay minerals. Appl Clay Sci 46:27–36

Dzombak DA, Morel FMM (1990) Surface complexation modelling: hydrous ferric oxide. Wiley, New York

Essington ME, Lee J, Seo Y (2010) Adsorption of antibiotics by montmorillonite and kaolinite. Soil Sci Soc Am J 74:1577–1588

Evanko CR, Dzombak DA (1999) Surface complexation modeling of organic acid sorption to goethite. J Colloid Interface Sci 214:189–206

Figueroa RA, Mackay AA (2005) Sorption of oxytetracycline to iron oxides and iron oxide-rich soils. Environ Sci Technol 39:6664–6671

Figueroa RA, Leonard A, Mackay AA (2004) Modeling tetracycline antibiotic sorption to clays. Environ Sci Technol 38:476–483

Goldberg S (2005) Inconsistency in the triple layer model description of ionic strength dependent boron adsorption. J Colloid Interface Sci 285:509–517

Gu XY, Evans LJ (2008) Surface complexation modelling of Cd(II), Cu(II), Ni(II), Pb(II) and Zn(II) adsorption onto kaolinite. Geochim Cosmochim Acta 72:267–276

Gu C, Karthikeyan KG (2008) Sorption of the antibiotic tetracycline to humic-mineral complexes. J Environ Qual 37:704–711

Gu C, Karthikeyan KG, Sibley SD, Pedersen JA (2007) Complexation of the antibiotic tetracycline with humic acid. Chemosphere 66:1494–1501

Gu XY, Evans LJ, Barabash SJ (2010) Modeling the adsorption of Cd (II), Cu (II), Ni (II), Pb (II) and Zn (II) onto montmorillonite. Geochim Cosmochim Acta 74:5718–5728

Herbelin AL, Westall JC (1999) FITEQL 4.0: a computer program for determination of chemical equilibrium constants from experimental data. Department of Chemistry, Oregon State University, Corvallis, Oregon

Hu XG, Luo Y, Zhou QX, Xu L (2008) Determination of thirteen antibiotics residues in manure by solid phase extraction and high performance liquid chromatography. Chin J Anal Chem 36:1162–1166

Ikhsan J, Johnson BB, Wells JD, Angove MJ (2004) Adsorption of aspartic acid on kaolinite. J Colloid Interface Sci 273:1–5

Ikhsan J, Angove MJ, Johnson BB, Wells JD (2005) Cosorption of Zn(II) and 2-, 3-, or 4-aminopyridine by montmorillonite. J Colloid Interface Sci 284:400–407

Ji LL, Chen W, Duan L, Zhu DQ (2009) Mechanisms for strong adsorption of tetracycline to carbon nanotubes: a comparative study using activated carbon and graphite as adsorbents. Environ Sci Technol 43:2322–2327

Jonsson CM, Persson P, Sjoberg S, Loring JS (2008) Adsorption of glyphosate on goethite (alpha-FeOOH): surface complexation modeling combining spectroscopic and adsorption data. Environ Sci Technol 42:2464–2469

Knapp CW, Dolfing J, Ehlert PAI, Graham DW (2010) Evidence of increasing antibiotic resistance gene abundances in archived soils since 1940. Environ Sci Technol 44:580–587

Kulshrestha P, Giese RF, Aga DS (2004) Investigating the molecular interactions of oxytetracycline in clay and organic matter: insights on factors affecting its mobility in soil. Environ Sci Technol 38:4097–4105

Landry CJ, Koretsky CM, Lund TJ, Schaller M, Das S (2009) Surface complexation modeling of Co(II) adsorption on mixtures of hydrous ferric oxide, quartz and kaolinite. Geochim Cosmochim Acta 73:3723–3737

Li ZH, Chang PH, Jean JS, Jiang WT, Wang CJ (2010a) Interaction between tetracycline and smectite in aqueous solution. J Colloid Interface Sci 341:311–319

Li ZH, Kolb VM, Jiang WT, Hong HL (2010b) FTIR and XRD investigations of tetracycline intercalation in smectites. Clay Clay Miner 58:462–474

Liu ZZ, He Y, Xu JM, Huang PM, Jilani G (2008) The ratio of clay content to total organic carbon content is a useful parameter to predict adsorption of the herbicide butachlor in soils. Environ Pollut 152:163–171

Lund TJ, Koretsky CM, Landry CJ, Schaller MS, Das S (2008) Surface complexation modeling of Cu(II) adsorption on mixtures of hydrous ferric oxide and kaolinite. Geochem Trans 9:9

Morton JD, Semrau JD, Hayes KF (2001) An X-ray absorption spectroscopy study of the structure and reversibility of copper adsorbed to montmorillonite clay. Geochim Cosmochim Acta 65:2709–2722

Parolo ME, Savini MC, Valles JM, Baschini MT, Avena MJ (2008) Tetracycline adsorption on montmorillonite: pH and ionic strength effects. Appl Clay Sci 40:179–186

Parolo ME, Avena MJ, Pettinari G, Zajonkovsky I, Valles JM, Baschini MT (2010) Antimicrobial properties of tetracycline and minocycline-montmorillonites. Appl Clay Sci 49:194–199

Pei ZG, Shan XQ, Kong JJ, Wen B, Owens G (2010) Coadsorption of ciprofloxacin and Cu(II) on montmorillonite and kaolinite as affected by solution pH. Environ Sci Technol 44:915–920

Pils JRV, Laird DA (2007) Sorption of tetracycline and chlortetracycline on K- and Ca-saturated soil clays, humic substances, and clay-humic complexes. Environ Sci Technol 41:1928–1933

Sarmah AK, Meyer MT, Boxall ABA (2006) A global perspective on the use, sales, exposure pathways, occurrence, fate and effects of veterinary antibiotics (VAs) in the environment. Chemosphere 65:725–759

Swedlund PJ, Webster JG, Miskelly GM (2009) Goethite adsorption of Cu(II), Pb(II), Cd(II), and Zn(II) in the presence of sulfate: properties of the ternary complex. Geochim Cosmochim Acta 73:1548–1562

Thiele-Bruhn S, Beck IC (2005) Effects of sulfonamide and tetracycline antibiotics on soil microbial activity and microbial biomass. Chemosphere 59:457–465

Wang YJ, Jia DA, Sun RJ, Zhu HW, Zhou DM (2008) Adsorption and cosorption of tetracycline and copper(II) on montmorillonite as affected by solution pH. Environ Sci Technol 42:3254–3259

Wang JT, Hu J, Zhang SW (2010) Studies on the sorption of tetracycline onto clays and marine sediment from seawater. J Colloid Interface Sci 349:578–582

Wilson CJ, Brain RA, Sanderson H, Johnson DJ, Bestari KT, Sibley PK, Solomon KR (2004) Structural and functional responses of plankton to a mixture of four tetracyclines in aquatic microcosms. Environ Sci Technol 38:6430–6439

Zhao Y, Geng J, Wang X, Gu X, Gao S (2011) Tetracycline adsorption on kaolinite: pH, metal cations and humic acid effects. Ecotoxicology 20:1141–1147

Zhao Y, Gu X, Gao S, Geng J, Wang X (2012) Adsorption of tetracycline (TC) onto montmorillonite: cations and humic acid effects. Geoderma 183:12–18

Zhao Y, Tong F, Gu X, Gu C, Wang X, Zhang Y (2014) Insights into tetracycline adsorption onto goethite: experiments and modeling. Sci Total Environ 470–471:19–25